

THE EVOLUTION OF DWARF GALAXIES WITH STAR FORMATION IN OUTWARD PROPAGATING SUPER SHELL

Masao Mori^{1,2}, Yuzuru Yoshii^{3,4}, Takuji Tsujimoto⁵ and Ken'ichi Nomoto^{1,4}

Received XX XXXXX 1996; accepted YY YYYYYY 1996

arXiv:astro-ph/9701052v2 13 Jan 1997

¹Department of Physics, School of science, Nagoya University, Chikusa-ku, Nagoya 464-01, Japan

²The Institute of Physical and Chemical Research(RIKEN), Wako, Saitama, 351-01, Japan

³Institute of Astronomy, Faculty of science, University of Tokyo, Mitaka, Tokyo 181, Japan

⁴Research Center for the Early Universe, School of science, University of Tokyo, Bunkyo-ku, Tokyo 113, Japan

⁵National Astronomical Observatory, Mitaka, Tokyo 181, Japan

⁶Department of Astronomy, School of science, University of Tokyo, Bunkyo-ku, Tokyo 113, Japan

ABSTRACT

We simulate the dynamical and chemical evolution of a dwarf galaxy embedded in a dark matter halo, using a three-dimensional N -body/SPH simulation code combined with stellar population synthesis. The initial condition is adopted in accord with a $10^{10}M_{\odot}$ virialized sphere in a 1σ CDM perturbation which contains 10% baryonic mass. A supersonic spherical outflow is driven by the first star burst near the center of the galaxy and produces an expanding super shell in which stars are subsequently formed. Consecutive formation of stars in the expanding shell makes the stellar system settled with the exponential brightness profile, the positive metallicity gradient, and the inverse color gradient in agreement with observed features of dwarf galaxies. We therefore propose that the energy feedback via stellar winds and supernovae is a decisive mechanism for formation of less compact, small systems like dwarf galaxies.

Subject headings: galaxies: formation – galaxies: structure – galaxies: abundances – cosmology: dark matter

1. Introduction

Our understanding of how galaxies originate and distribute on large scales in the universe has greatly improved in the last two decades. While the standard model of hierarchical galaxy clustering (White & Rees 1978) has been successful in explaining the clustering pattern of galaxies revealed by redshift surveys, it predicts a large number of low-mass galaxies ($L < 10^{10}L_{\odot}$) beyond that estimated from the observed luminosity function of galaxies (White & Frenk 1991; Cole *et al.* 1994). The hierarchical model should therefore involve some mechanism which suppresses the formation of such small galaxies. Main mechanisms so far proposed include an energy feedback from supernovae that prevents the collapse of a forming galaxy (Dekel & Silk 1986; Lacey & Silk 1992) and a photoionization by ultraviolet background radiation that keeps the gas hot and unable to collapse (Dekel & Rees 1987; Efstathiou 1992).

Significant body of new observations of nearby dwarf galaxies has revealed a web of filaments, loops and expanding super giant shells which are imprinted in the ionized gas around individual galaxies (Meurer, Freeman & Dopita 1992; Marlowe, Heckman & Wyse 1995; Hunter 1996). Since the traces of energetic winds are oriented from supernovae or massive stars, it is evident that the heat input from them greatly affects the dynamics of small galaxies. This feedback of energy into the interstellar medium must play a decisive role in the early stage of galaxy evolution when star formation rate is expected to be much higher.

Dekel & Silk (1986) showed that the supernova feedback mechanism nicely accounts for the observed correlations between metallicity, color and luminosity of galaxies (see also Vader 1986; Yoshii & Arimoto 1987). There is however a clear distinction in structural and chemical quantities between dwarf ellipticals (dEs) and normal ellipticals in spite of their morphological similarity. The central concentration of dEs is relatively low and their

luminosity profiles are best fitted by an exponential function, whereas the profiles of normal ellipticals are known to follow de Vaucouleurs' law (Faber & Lin 1983; Binggeli, Sandage & Tarenghi 1984; Ichikawa, Wakamatsu & Okamura 1986; Caldwell & Bothun 1987). Moreover, the color of many dEs becomes redder towards outer radii of the system (Vader *et al.* 1988; Kormendy & Djorgovski 1989; Chaboyer 1994), and this trend of color gradient is clearly opposite to normal galaxies. The origin of these striking features of dEs remains yet to be explained (for a review see Ferguson & Binggeli 1994). In particular, no attempts have ever been made to examine whether the supernova feedback mechanism is viable also in this context.

In this paper, we use three dimensional simulation code with a cosmologically motivated initial condition and investigate the formation and evolution of a dE galaxy taking into account the dynamical responses of the system from supernova-driven winds. Our simulation shows that such winds propagating outwards from inside the system collide with the infalling gas and produce the super shell in which stars are formed. This specific process of star formation turns out to reproduce the observed features of dEs, and therefore the heating by supernovae proves to be an ideal suppressing mechanism against the efficient formation of low-mass galaxies in the hierarchical clustering model.

2. Numerical Method

Our simulation uses a hybrid N -body/hydrodynamics code which is applicable to a complex system consisting of dark matter, stars and gas. The gas is allowed to form stars and is subject to physical processes such as the radiative cooling and the energy feedback from supernovae and massive stars. The cooling rate of the gas is calculated assuming the primordial composition, and the effect of photoionization by ultraviolet background radiation is ignored for simplicity. Chemical and photometric evolution of the system can

also be simulated by this code. The collisionless dynamics for dark matter particles and stars is treated by the N -body method and the gas dynamics by the method of smoothed particle hydrodynamics (SPH) (Hernquist & Katz 1989; Monaghan 1992). Our numerical technique is essentially similar to that adopted by Steinmetz (1996). We only briefly describe how to calculate the self-gravity, star formation, and energy feedback. The details will be given in a forthcoming paper (Mori *et al.* 1996b).

Self-gravity calculations are run on the hardware GRAPE-3AF (Sugimoto *et al.* 1990) by using the “Remote-GRAPe” system. This remote system is newly developed in order to allow an access to the GRAPE-3AF from local workstations which are not physically connected to the host workstation. Thus, self-gravity calculations can be performed in parallel with other calculations, so that the calculation time is considerably shortened. The performance analysis of this system is reported by Nakasato *et al.* (1996) and Mori *et al.* (1996b).

Stars are assumed to form in rapidly cooling, Jeans unstable and converging regions at a rate which is inversely proportional to the local dynamical time (Katz 1992; Navarro & White 1993; Steinmetz & Müller 1994). When a star particle is formed, we identify this with approximately 10^4 single stars and distribute the associated mass of the star particle over the single stars according to Salpeter’s (1955) initial mass function. The lower and upper mass limits are taken as $m_l = 0.1M_\odot$ and $m_u = 50M_\odot$, respectively.

Our SPH algorithm for treating the energy feedback from massive stars is a more physically motivated one and is different from those adopted by previous authors (Katz 1992; Navarro & White 1993; Mihos & Hernquist 1994). When a star particle is formed and identified with a stellar assemblage as described above, stars more massive than $8 M_\odot$ start to explode as Type II supernovae (SNe II) with the explosion energy of 10^{51} ergs and their outer layers are blown out with synthesized metals leaving the remnant of $1.4 M_\odot$.

We can regard this assemblage as continuously releasing the energy at an average rate of 8.44×10^{35} ergs sec^{-1} per star during the explosion period from $t(m_u) = 5.4 \times 10^6$ yrs until $t(8M_\odot) = 4.3 \times 10^7$ yrs where $t(m)$ is the lifetime of a star of mass m . Prior to the onset of SN explosions, however, their progenitors develop stellar winds and also release the energy of 10^{50} ergs into the interstellar medium at an average rate of 7.75×10^{34} ergs sec^{-1} per star. Consequently, once a new star particle is formed, the energy from stellar winds is supplied to the gas particles within a sphere of radius R_{snr} , and the energy, metals and material from SNe II are subsequently supplied to the same region. The radius R_{snr} is set equal to the maximum extension of the shock front in the adiabatic phase of supernova remnant and is given by $R_{snr} = 32.9 E_{51}^{1/4} n^{-1/2}$ pc (Shull & Silk 1979) where E_{51} is the released energy in units of 10^{51} ergs and n is the number density of the gas in units of cm^{-3} which surrounds the star particle. The gas within R_{snr} remains adiabatic until multiple SN phase ends at $t(8M_\odot)$, and then it cools according to the adopted cooling rate of the gas. We compute the chemical evolution using the new calculations of stellar nucleosynthesis products (Tsujimoto *et al.* 1995).

3. Simulation Result

Following a standard model of the cold dark matter (CDM) universe ($\Omega_0 = 1$, $H_0 = 50$ $\text{km sec}^{-1} \text{Mpc}^{-1}$), we consider a less massive protogalaxy as a gas sphere with mass of $10^9 M_\odot$ embedded in a 1σ density peak having a total mass of $10^{10} M_\odot$ with a baryon to dark matter ratio equal to 1/9. The distribution of dark matter halo is assumed to have a King profile with the central concentration index of $c = 1$. This two-component system is made to settle in a virial equilibrium from which the gas temperature and the velocity dispersion of dark matter are estimated as an initial condition. Our simulation uses 10^4 particles for each of gas and dark matter particles. The gravitational softening parameter

is adopted as 78.9 pc for gas particles and 36.6 pc for collisionless particles.

As soon as we start a simulation, the gas in the central region of the protogalaxy rapidly cools and begins to contract owing to the self-gravity of dark matter and gas. When the gas temperature becomes close to $10^4 K$ and stops decreasing, a quasi-isothermal contraction is established. A further increase of the gas density causes a burst of star formation in the central region. Thereafter, as massive stars explode as SNe II, the surrounding gas acquires the thermal energy and the gas temperature rises up to about $10^6 K$. At the same time, the gas is gradually polluted with synthesized metals from SNe II. About 5% of the initial gas mass is used up in this formation of the first generation stars.

The shock waves propagate outwards and the supernova-driven spherical outflow occurs from inside. This outflow collides with the infalling gas and the high-density super shell is eventually formed. While the gas is continuously swept up by the super shell, the gas density further increases due to the enhanced cooling rate in the already dense shell. Then the intense formation of stars begins within the super shell, and subsequent SN explosions further accelerate the outward expansion of the shell. Star formation continues in the expanding shell for about 10^8 yrs until the gas density in the shell becomes too low to form new stars. About 26% of the initial gas mass is turned into stars in this stage. The remaining gas in the shell is blown out to the intergalactic space at supersonic speed. The ejected gas has already enriched to the yield value $y_Z \approx Z_\odot$ having the metal abundance of $\log Z/Z_\odot \sim 0.0$. Figure 1 shows the ring-like distribution of gas particles and newly born star particles near the $X - Y$ sectional plane at the elapsed time of $\sim 2 \cdot 10^7$ yrs in the simulation. It is evident from this figure that the star-forming site is well confined in the shell.

In such a way, a total of about 31% of the initial gas mass has turned into stars before the dwarf galaxy is formed. The baby stars initially have the velocity vectors of the gas

from which the stars are formed. Therefore, the first generation stars have zero systematic velocity, but the later generation stars has a large outward radial velocity component. The oscillation of swelling and contraction of the system continues for several 10^8 yrs, and the system becomes settled in a quasi-steady state in $3 \cdot 10^9$ yrs. The resulting stellar system forms a loosely bound virialized system due to the significant mass loss and has a large velocity dispersion and a large core. Consequently the surface mass distribution is approximately exponential (Figure 2a) and differs from the de Vaucouleur’s profile which is more concentrated towards the galaxy center. In order to enable a more direct comparison with the observation, we have computed the photometric evolution up to 10 Gyrs based on the method of stellar population synthesis, using the updates of stellar evolutionary tracks compiled by Kodama & Arimoto (1996). The resulting surface B -band brightness distribution at 10 Gyrs is obviously exponential (Figure 2b). The effective radius within which a half of the total light is contained is 1.42 kpc. The integrated blue luminosity of the system is $M_B = -14.5$ mag.

Stars are formed for the most part before the gas is fully polluted to the yield value $y_Z \approx Z_\odot$ of the synthesized metals. The average metal abundance of the stars in the system is as low as $\log Z/Z_\odot \sim -1.74$. This metallicity is consistent with a range covered by the observations, but is much lower than those of normal galaxies (Dekel & Silk 1986; Yoshii & Arimoto 1987). One outstanding feature discovered by our simulation is that the radial distribution of metal abundance in this system has a *positive* gradient (Figure 2c) which is in sharp contrast to the observed negative gradient for massive galaxies (Carollo, Danziger & Buson 1993). We note that the star-forming site moves outwards with the expanding shell and the gas in this shell is gradually enriched with synthesized metals from SNe II. Stars of later generations are necessarily born at larger radii with larger metallicities, leading to emergence of the positive metallicity gradient in the resulting stellar system.

Since the $V - K$ color sensitively traces the metallicity of underlying stellar population (Yoshii & Arimoto 1991), we calculate the radial distribution of the integrated $V - K$ color (Figure 2d), and the result is consistent with the observed trend of the inverse color gradient for dwarf galaxies (Vader *et al.* 1988; Kormendy & Djorgovski 1989; Chaboyer 1994).

4. Summary & Discussion

A three-dimensional N -body/SPH simulation code, combined with stellar population synthesis, is used to follow the dynamical and chemical evolution of a dwarf protogalaxy with $10^{10} M_{\odot}$ (baryonic/dark=1/9) which originates from a 1σ CDM perturbation. This less massive galaxy receives significant dynamical responses from the heat input by stellar winds and supernovae.

The first star burst near the center of the system produces a supersonic spherical outflow of the gas. This outflow collides with the infalling gas and gives rise to an expanding dense shell. Then, stars begin to form in the expanding shell with its site propagating outwards with the shell. We find from the simulation that this consecutive process of star formation creates the exponential brightness profile and the inverse color gradient of the system in agreement with the observations of dwarf galaxies.

Athanassoula (1994) performed one-dimensional simulations of the dynamical evolution of dE galaxies including the energy feedback from supernovae. The models without dark halo are shown to give a better agreement with observations than those with dark halo. Our more realistic, three-dimensional simulations however indicate that the dark halo is necessary and plays a vital role to form the bound stellar system, otherwise the system is blown out to disrupt completely.

In general, the color gradient of galaxies is created by the gradient in either metallicity

or age of the underlying stellar population. Simple models of chemical evolution of galaxies usually predict the negative metallicity gradient which corresponds to the color becoming redder towards the galaxy center. Since dwarf galaxies have the inverse color gradient, Vader *et al.* (1988) were led to interpret this observed trend in terms of the positive age gradient. We note however that stars with very low metallicities must have been formed on very short timescales and therefore no appreciable age difference results.

The above puzzling situation indicates that previous results based on simple models of chemical evolution can not be applied to small systems like dwarf galaxies. We demonstrate in this paper that dynamical modelling is the only proper way to investigate the evolution of dwarf galaxies. Successful reproduction of their basic features in our simulation suggests that the stellar energy feedback mechanism is indeed a likely mechanism against the efficient formation of low-mass galaxies in the CDM universe.

We are grateful to T. Shigeyama and M. Chiba for many fruitful discussions, to T. Kodama for providing us the tables of population synthesis prior to the publication, and to N. Nakasato for preparing the Remote-GRAPe library. This research has been supported in part by the Grant-in-Aid for Scientific Research (05242102, 06233101) and Center-of-Excellence Research (07CE2002) of the Ministry of Education, Science, and Culture in Japan.

REFERENCES

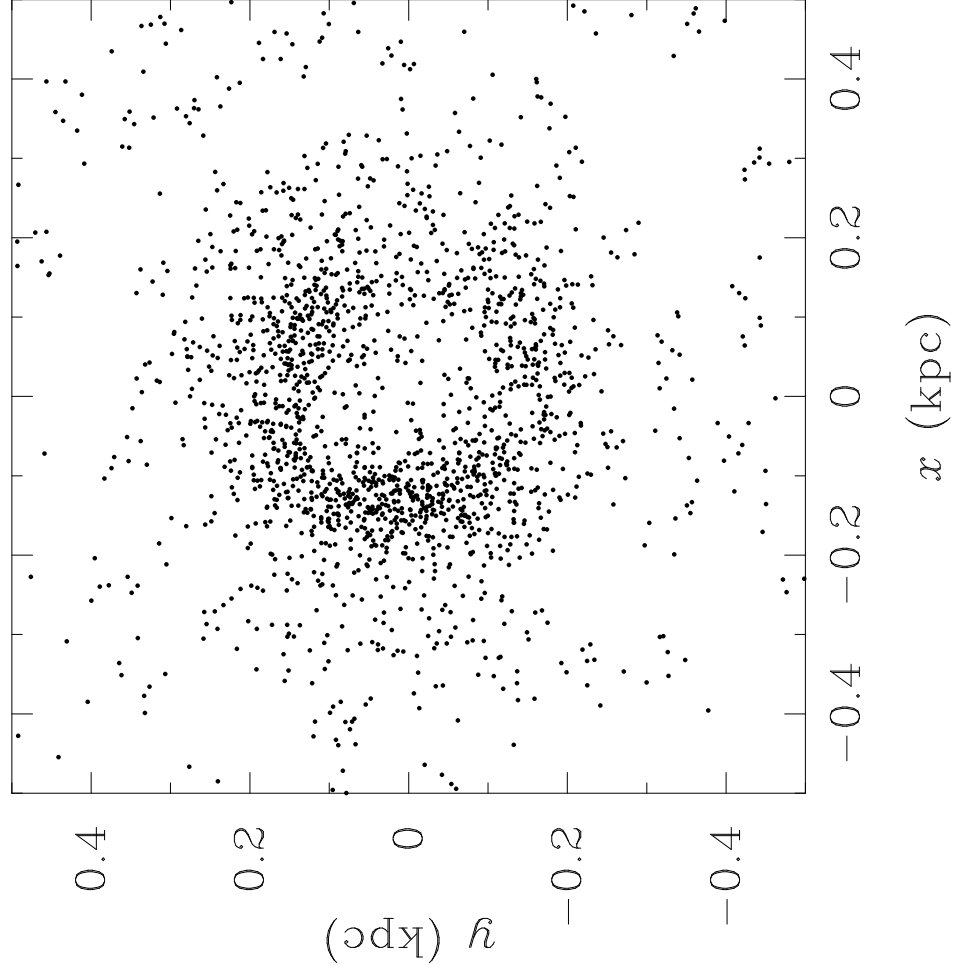
- Athanassoula, E., 1994, in *ESO/OHP Workshop on Dwarf Galaxies.*, eds. Meylan, G. & Prugniel, P., ESO, Garching, 525
- Binggeli, B., Sandage A., & Tarenghi, M., 1984, *AJ*, 89, 64
- Caldwell, N., & Bothun, G.D., 1987, *AJ*, 94, 1126
- Carollo, C.M., Danziger, I.J., & Buson, L., 1993, *MNRAS*, 265, 553
- Chaboyer, B., 1944, in *ESO/OHP Workshop on Dwarf Galaxies.*, eds. Meylan, G. & Prugniel, P., ESO, Garching, 485
- Cole, S., Aragón-Salamanca, A., Frenk, C.S., Navarro, J.F., & Zepf, S.E., 1994, *MNRAS*, 271, 781
- Dekel, A., & Rees, M.J., 1987, *Nature*, 326, 455
- Dekel, A., & Silk, J., 1986, *ApJ*, 303, 39
- Efstathiou, G., 1992, *MNRAS*, 256,43P
- Faber, S.M., & Lin, D.M.C., 1983, *ApJ*, 266,L17
- Ferguson, H.C., & Binggeli, B., 1994, *A&A Rev.*, 6, 67
- Hernquist, L., & Katz, N., 1989, *ApJS*, 70, 419
- Hunter, D.A., 1996, *ApJ*, 457, 671
- Ichikawa, S., Wakamatsu, K., & Okamura, S., 1986, *ApJS*, 60, 475
- Katz, N., 1992, *ApJ*, 391, 502
- Kodama, T., & Arimoto, N., 1996, *A&A*, in press
- Kormendy, J., & Djorgovski, S., 1989, *ARA&A*, 27, 235
- Lacey, C., & Silk, J., 1991, *ApJ*, 381, 14

- Marlowe, A.T., Heckman, T.M., & Wyse, R.F.G., 1995, ApJ, 438, 563
- Meurer, G.R., Freeman, K.C., & Dopita, M.A., 1992, AJ, 103, 60
- Mihos, J.C., & Hernquist, L., 1994 ApJ, 437, 611
- Monaghan, J. J., 1992, ARA&A, 30, 543
- Mori, M., Yoshii, Y., Tsujimoto, T., & Nomoto, K., 1996b, in preparation
- Nakasato, N., Mori, M., & Nomoto, K., 1996, ApJ, submitted
- Navarro J. F., & White, S. D. M., 1993, MNRAS, 265, 271
- Salpeter E. E., 1955, ApJ, 121, 161
- Shull, J.M., & Silk, J., 1979, ApJ, 234, 427
- Steinmetz, M., 1996, MNRAS, 278, 1005
- Steinmetz, M., & Müller, E., 1994, ApJ, 281, L97
- Sugimoto, D., Chikada Y., Makino J., Ito T., Ebisuzaki T., & Umemura M., 1990, Nature, 345,33
- Tsujimoto, T., Nomoto, K., Yoshii, Y., Hoshimoto, M., Yanagida, S., & Thielemann F.-K., 1996, MNRAS, 277, 945
- Vader, J.P., 1986, ApJ, 305, 669
- Vader, J.P., Vigroux, L., Lachièze-Rey, M., & Souviron J., 1988, A&A, 203, 217
- White, S.D.M., & Frenk, C.S., 1991, ApJ, 379, 52
- White, S.D.M., & Rees, M.J., 1978, MNRAS, 183, 341
- Yoshii, Y., & Arimoto, N., 1987, A&A, 188, 13
- Yoshii, Y., & Arimoto, N., 1991, A&A, 248, 30

Fig. 1.— Distribution of gas and star particles near the $X - Y$ sectional plane ($|X| \leq 0.5$ kpc, $|Y| \leq 0.5$ kpc, $|Z| \leq 0.05$ kpc). *Left panel:* snapshot for gas particles at the elapsed time of $2.17 \cdot 10^7$ yrs. *Right panel:* snapshot for newly born star particles between $2.05 \cdot 10^7$ yrs and $2.17 \cdot 10^7$ yrs.

Fig. 2.— Various simulated quantities as a function of radial distance away from the center of the bound stellar system at the elapsed time of 10 Gyrs. All the radial profiles are plotted against the radius in units of kpc (solid lines) or a quartic root of the radius (dotted lines). (a) Surface stellar mass density. (b) Surface B -band brightness. (c) Logarithmic stellar metal abundance. (d) Integrated $V - K$ color.

Gas particles



Baby-star particles

